COMPDYN 2011
3rd ECCOMAS Thematic Conference on
Computational Methods in Structural Dynamics and Earthquake Engineering
M. Papadrakakis, M. Fragiadakis, V. Plevris (eds.)
Corfu, Greece, 25–28 May 2011

PREDICTION OF SEISMIC RESPONSE PARAMETERS OF TYPICAL MASONRY BUILDING WITH CONSIDERATION OF EPISTEMIC UNCERTAINTIES

Jure Snoj[1], **Matjaž Dolšek**[1]

[1] University of Ljubljana, Faculty of Civil and Geodetic Engineering, Jamova 2, Ljubljana, Slovenia
e-mail: jure.snoj@fgg.uni-lj.si; mdolsek@ikpir.fgg.uni-lj.si

Keywords: Seismic risk; Masonry structure; Epistemic uncertainty; Latin hypercube sampling; Pushover analysis; IN2.

ABSTRACT. *The seismic risk assessment of structures is a complex problem, which combines seismic hazard analysis, structural vulnerability analysis and analysis of socio-economic impacts. In addition, seismic risk assessment, especially in the case of old masonry buildings, is subject to many uncertainties, not only due to the random nature of earthquakes but also due to physical and modeling uncertainties related to prediction of structural vulnerability. Recent studies have shown that epistemic (modeling) uncertainties can significantly affect seismic response parameters. However, uncertainty analysis usually involves simulations, and it is therefore computationally extremely demanding, especially if seismic response parameters are computed by using nonlinear dynamic analysis. Therefore, simplified nonlinear seismic performance assessment method is used to estimate seismic response parameters for a set of structural models, which are determined by utilizing the Latin Hypercube Sampling technique. The proposed method is demonstrated by means of an example of two masonry buildings, which are modeled and analyzed by using the computer program Tremuri. Results of the study indicate that the effects of epistemic uncertainties, in addition to aleatoric uncertainties, are significant.*

1 INTRODUCTION

A substantial part of built environment is represented by masonry buildings, which were mainly constructed in the past and are therefore not earthquake resistant structures. Consequently, earthquakes endanger this part of built environment and human lives more than thought. In order to contribute to the mitigation of seismic risk, advanced methods and tools should be developed, which will enable well-informed decision making, this being the key element for the future protection of built environment against earthquakes.

Probably the simplest closed-form solution for seismic risk assessment of structures expressed in terms of the mean annual frequency of exceeding a given limit state was proposed by Cornell et al. [1]. However, the most demanding part of the risk assessment procedure, i.e. the incremental dynamic analysis (IDA) [2], which enables direct evaluation of the record-to-record variability in structural response through a set of ground motion records, can be replaced with the IN2 analysis [3, 4]. These methods were applied in the study presented in the paper. However, several methods for estimating seismic risk of masonry structures exist. For example, a methodology for deriving analytical fragility curves for masonry buildings based on stochastic nonlinear analyses was introduced [5]. The method involves consideration of aleatoric and epistemic uncertainty since the nonlinear static (pushover) analyses are used to define the probability distributions of each damage state with consideration of epistemic uncertainties, while the incremental dynamic analysis for a set of ground motion records is performed to determine the probability density function of the displacement demand.

The effects of epistemic uncertainties are usually not explicitly considered for assessment of seismic risk of structure since this task is computationally demanding and requires sophisticated software tools. Therefore, only approximate methods for seismic performance assessment of structures with consideration of epistemic uncertainties can be adopted for practical purposes. Such a method, which combines the IN2 [3, 4] and a set of structural models determined by utilizing the variant of Latin Hypercube Sampling (LHS) technique [6], is presented in this paper. In its first part the method is briefly summarized, while in the second part its use is demonstrated by means of two examples of three-storey buildings, which were analyzed by structural analysis program - Tremuri [7].

2 SEISMIC RISK ASSESSMENT METHOD

Seismic risk of a building can be, in its most basic formulation, estimated with the mean annual frequency of exceeding a defined limit state (LS), which can be determined as follows:

$$P_{\mathrm{LS}} = \int_0^{\infty} P\left(LS \middle| I_M = i_m\right) \cdot \left| \frac{dH\left(i_m\right)}{di_m} \right| \cdot di_m \tag{1}$$

where $P\left(LS \middle| I_M = i_m\right)$ is the probability of exceeding limit state (LS) if the intensity measure I_{M} is equal to i_{m}. Hazard function $H(i_m)$ is usually expressed in terms of mean annual frequency that the intensity measure I_{M} will be larger or equal to i_{m} and can be approximated as [1]:

$$H\left(i_m\right) = k_o \left(i_m\right)^{-k} \tag{2}$$

According to this assumption it follows, that the hazard function is linear in log-log coordinates.

The formulation of the seismic risk according to Eq.(1) is the so called IM-based formulation and requires definition of the intensity measure (i_{m}), which is the peak ground accelera-

tion (a_g) in the case of this study. Cornell had shown that mean annual frequency of exceeding given limit state can be, according to Eqs. (1) and (2) expressed as follows:

$$\lambda_{\mathrm{LS}} = H\left(\tilde{a}_{g,LS}\right)\cdot e^{\frac{1}{2}\cdot k_{LS}^2\cdot\beta_{LS}^2} = k_o\cdot\left(\tilde{a}_{g,LS}\right)^{-k_{LS}}\cdot e^{\frac{1}{2}\cdot k_{LS}^2\cdot\beta_{LS}^2} \tag{3}$$

where $\tilde{a}_{g,LS}$ is the median value of the IM-based capacity (i.e. the median peak ground acceleration which causes the given limit state), β_{LS} is the corresponding standard deviation of natural logarithms and k_{LS} is the slope of the hazard curve, which has to be estimated for each limit state.

Many different procedures exist, which can be used in order to estimate the fragility parameters $\tilde{a}_{g,LS}$ and β_{LS}. For example, the parametric analysis method IDA, which involves the nonlinear dynamic analysis for a set of ground motion records scaled to different levels of defined intensity measure, is probably the most accurate procedure for determination of fragility parameters. However, it is computationally extremely demanding, especially, if IDA is extended by the set of structural models in order to consider effects of epistemic uncertainties [8]. Two alternative, practice-oriented approaches are the approximate IDA performed by using an equivalent single-degree-of-freedom (SDOF-IDA) model [9] and the N2 method [3,4].

The approximate IDA is more accurate, since both fragility parameters can be evaluated by taking into account the record-to-record variability. The N2 method, which was used in the paper, provides mean estimates for limit-state intensities (e.g. peak ground acceleration corresponding to limit state - $a_{g,LS}$) with respect to record-to-record variability (aleatoric uncertainty), but its dispersion has to be predetermined or assumed. Since λ_{LS} is estimated based on the median $\tilde{a}_{g,LS}$, it was conservatively assumed that $\overline{a}_{g,LS} \approx \tilde{a}_{g,LS}$.

In addition to aleatoric uncertainty, the epistemic uncertainties can also significantly affect the fragility parameters. They are knowledge-based and are most often related to the physical properties of the structure and its modelling parameters. In this study epistemic uncertainties are treated by using the LHS technique [6], which is summarized in the Section 2.1. The result of the LHS technique is N_{sim} structural models and consequently N_{sim} peak ground accelerations corresponding to predetermined limit state are obtained.

The median $\tilde{a}_{g,LS}$ and the dispersion β_{LS} in general depends on the method used for their estimation. In the case of this study the fragility parameters were estimated according to the method of moments, as follows:

$$\tilde{a}_{g,LS} = \overline{a}_{g,LS}\cdot e^{-0.5\cdot\beta_{LS}^2} \tag{4}$$

$$\beta_{LS} = \sqrt{\ln\left(\frac{\sigma^2}{\overline{a}_{g,LS}^2}+1\right)} \tag{5}$$

where $\overline{a}_{g,LS}$ and σ^2 are the sample mean and corresponding variance. In addition to LHS method, which is briefly summarized in next section, a procedure for determining the equivalent SDOF model, which is employed for estimation of the fragility parameters, is also briefly described in the Section 2.2.

2.1 Summary of the Latin Hypercube Sampling technique

The Latin Hypercube Sampling technique [10] uses stratification of the probability distribution function of the random variable X_i, therefore it requires fewer simulations as Monte Carlo method. Within the proposed methodology, the efficient LHS technique, which was re-

cently proposed by Vořechovský and Novák [6], is used and it can be applied for any probability distribution of random variables and the target correlation matrix.

The sample matrix can be calculated in two steps. In the first step, each random variable is sampled using N_{sim} values, which is shown in Figure 1. Firstly, the codomain of the cumulative distribution function is divided into k intervals, each having the length of $1/N_{sim}$. The k-th sample value of the i-th random variable ($x_{i,k}$) is determined based on the mean probability related to each interval as follows:

$$x_{i,k} = \frac{\int_{a_{i,k-1}}^{a_{i,k}} x \cdot f_{Xi}(x)\,dx}{\int_{a_{i,k-1}}^{a_{i,k}} f_{Xi}(x)\,dx} = N_{Sim} \cdot \int_{a_{i,k-1}}^{a_{i,k}} x \cdot f_{Xi}(x)\,dx \tag{6}$$

where $f_{Xi}(x)$ is the probability density function of the random variable X_i, while $a_{i,k-1}$ and $a_{i,k}$ are the values of random variable X_i, which correspond, respectively, to the probability at the lower and the upper range of the k-th interval (Figure 1). Boundaries of the interval are estimated as follows:

$$a_{i,k} = F_{Xi}^{-1}\left(\frac{k}{N_{sim}}\right) \tag{7}$$

where $f_{Xi}(x)$ is the inverse of the cumulative distribution function of the random variable X_i.

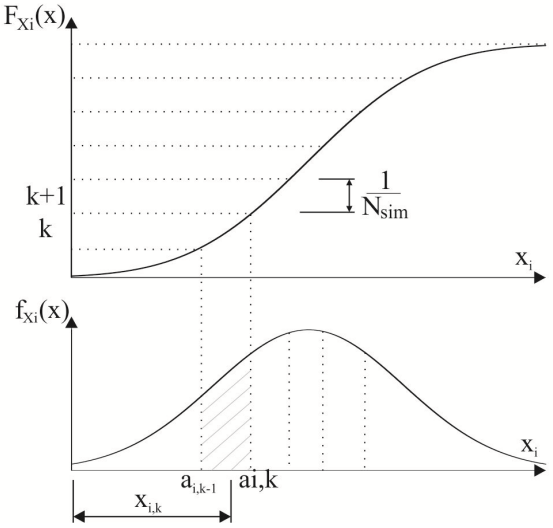

Figure 1: Sampling of random variable X_i according to the Latin Hypercube Sampling technique.

Such sampling is more accurate with respect to the sampling based on the probabilities in the middle of equidistant intervals since the influence of the data in the tails of probability density function on the variance is smaller [6].

Especially in the case of very small number of samples, undesired correlation can occur between random variables. In this case generated correlation matrix **S** significantly deviates from the prescribed (target) correlation matrix **K**. The difference between **S** and **K** is minimized by using the stochastic optimization method called "simulated annealing". It was first used in metallurgy and has some advantages, since its algorithm is very robust and it makes it possible to search for a global minimum.

In order to formulate the optimization problem, a suitable measure for difference between correlation matrices has to be defined. In the case of discussed problem, the norm E which takes into account deviations of all correlation coefficients simultaneously, is a good fitness function, which can be minimized by permutation of elements in sample matrix **X**. It is defined as follows:

$$E = \frac{2}{N_{\text{var}}\left(N_{\text{var}}-1\right)}\sqrt{\sum_{i=1}^{N_{\text{var}}-1}\sum_{k=i+1}^{N_{\text{var}}}\left(S_{\text{i,k}}-K_{\text{i,k}}\right)^2} \tag{8}$$

where $S_{i,k}$ and $K_{\text{i,k}}$ are the coefficients of the generated and target correlation matrix, respectively, and N_{var} is the number of random variables X_i.

Optimization is an iterative procedure, where each iteration consists of two steps: mutation and selection. Mutation represents the change of the ranks of two randomly selected elements of random variable X_i, while selection makes it possible to decide if the new arrangement of the random variable X_i is acceptable or not. According to the simulated annealing algorithm, the new arrangement is automatically accepted if it results in a decrease of the norm E, otherwise new arrangement is accepted only if the random variable Z, which is defined in Eq. (9), is positive.

$$Z = e^{-\frac{\Delta E}{T}} - R \tag{9}$$

where ΔE is the difference in norms E before and after random change of the ranks, R is uniformly distributed random variable in the interval [0,1] and T is the so-called temperature, which comes from annealing in metallurgy. Note that the initial temperature has to be defined in the algorithm and it is decreased step by step after a certain number of mutations, by using a reduction factor, which has the value 0.95, as recommended in [6].

The result of the optimization is optimized sample matrix **X**, which has N_{sim} rows and its' i-th row represents i-th structural model.

2.2 The equivalent SDOF model

In this Section the definition of the equivalent SDOF model, which is determined based on the results of the pushover analysis, is briefly described. More details regarding the definition of the equivalent SDOF model can be found elsewhere [4].

It is defined that the lateral loads used in the pushover analysis correspond to the product of mass matrix **M** and the vector $\boldsymbol{\phi}$ related to assumed deformation shape, which has the value 1 at the location of the top displacement ($\varphi_n = 1$), and is assumed proportional to the first mode shape. In this case, the pushover curve corresponding to the equivalent SDOF model (F^* and m^*) is determined based on the pushover curve of the structural model by dividing the base shear F and top displacement D with the transformation factor Γ, which is defined as follows:

$$\Gamma = \frac{m^*}{\sum_{i=1}^{n} m_i\phi_i^2},\quad m^* = \sum_{i=1}^{n} m_i\phi_i \tag{10}$$

where m_i and φ_i are masses and normalized deformations at the location of the i-th storey, and m^* is the mass of the equivalent SDOF model. The pushover curve of equivalent SDOF model has to be idealized with suitable force-displacement relationship. The corresponding initial stiffness (F_y^* / D_y^*) and the mass of the equivalent SDOF model define its period:

$$T^* = 2\pi\sqrt{\frac{m^* D_y^*}{F_y^*}} \tag{11}$$

where F_y and D_y are, respectively, yield force and yield displacement of the equivalent SDOF model.

3 EXAMPLE

The proposed methodology is demonstrated by means of seismic risk assessment of two three storey masonry buildings. Fragility parameters are estimated with approximate procedure involving N2 method. Results of both buildings are compared and the influence of epistemic uncertainties is discussed.

3.1 Description of the structures and structural models

The first example structure is a three-storey unreinforced masonry building A (Figures 2, 3 - left), which was selected from literature [11]. This building is symmetric around the Y axis and has 5.3 % of shear walls in the Y direction and 5.6 % shear walls in the X direction. Wall thickness is equal to 30 cm and storey height of all floors is equal to 2.8 m.

The second three-storey structure (building B, Figures 2, 3 - right) was derived from the geometry of SPEAR building [12], which was transformed into masonry building by adopting wall thickness equal to 30 cm, which amounted to 7.8 % of shear walls in X direction and 8.1 % walls in Y direction. The height of the first floor of the building B is 2.75 m, while the height of other stories is 3 m.

Both buildings have concrete slabs, which are considered as rigid diaphragms. At each floor level of both buildings, all walls are connected with continuous concrete beams with depth of 30 cm, which are reinforced with four 16 mm rebar (two at the bottom and two at the top) and 2 leg stirrups with 6 mm diameter at 25 cm spacing.

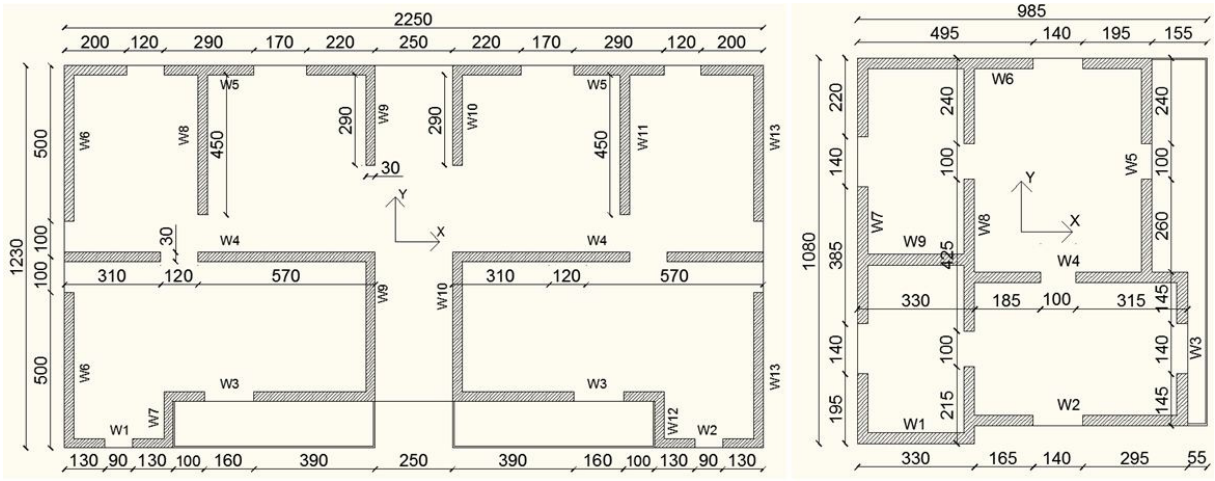

Figure 2: The plan of the building A (left) and building B (right)

Models of both buildings were made by using program 3Muri [13], specialized for seismic analysis and performance assessment of masonry structures, while the analysis was performed by using research version of the same program, Tremuri, which was developed at the University of Genoa [7]. The program is based on effective macro-element approach and enables accurate modelling, nonlinear pushover and time history analysis of masonry

buildings at very small computational burden [14]. Program models nonlinear behaviour of masonry piers and lintels with flexural and shear hinges, defined by a bilinear ideally elasto-plastic moment-rotation or force-displacement relationship, where ultimate drifts are defined for sliding shear mechanism (δ_s) and for flexural collapse mechanism (δ_f).

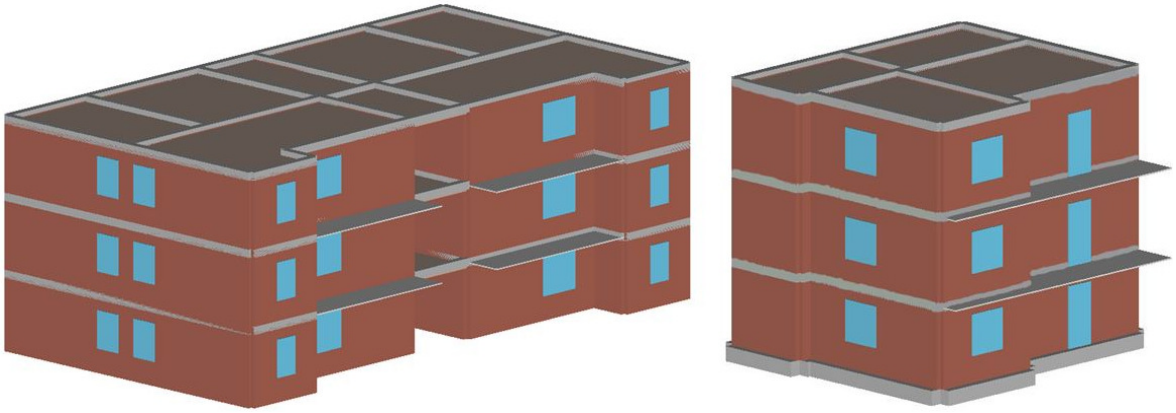

Figure 3: 3D view of the model A (left) and model B (right)

The vertical loads for both buildings, considered in the pushover analysis, are presented in the Table 1. Note that the live load was combined with the self weight by assuming combination factors 0.3 on the roof and 0.15 elsewhere.

Type of load	Building A	Building B
Self weight of masonry walls	16 kN/m^3	16 kN/m^3
Self weight and dead load of floors	5 kN/m^2	4.3 kN/m^2
Self weight and dead load of balconies	5 kN/m^2	4.3 kN/m^2
Self weight and dead load of staircase	5 kN/m^2	5 kN/m^2
Live load on floors	2 kN/m^2	2 kN/m^2
Live load on the staircase and balconies	4 kN/m^2	2.5 kN/m^2

Table 1: The self weight and the live loads used for definition of vertical load on the structure.

3.2 Uncertain parameters

In the case of this study some material and modelling parameters were considered uncertain. These parameters are: Young's modulus E, shear modulus G, compression strength of masonry wall f_m, initial shear strength f_{v0}, friction coefficient μ, nonlinear deformability parameter G_c, softening parameter β and ultimate drift ratios δ_s and δ_f that correspond to the shear and flexural collapse of masonry element, respectively.

The mean values of the uncertain parameters and corresponding coefficients of variation were adopted from literature [5] due to the lack of our own experimental data and are presented in Table 2. Normal distribution was assumed for all random variables.

Majority of the correlation coefficients between random variables was assumed 0. However, correlation coefficients between E, G, f_m, f_{vk0} were determined based on experimental data [15].

The optimized sample matrix $\mathbf{X}$ was determined according to the LHS technique, described in section 2.1, by assuming N_{sim} = 30. The norm E has a very low value of 0.0005 and the maximum difference between optimized and prescribed correlation matrix component is only 0.01. Therefore it was assumed, that the sample of uncertain parameters is appropriate for further analysis, although it cannot be claimed that the size of the sample is large enough in order to guarantee prediction of seismic response parameters with sufficient accuracy.

Thirty structural models were generated, since i-th row in optimized sample matrix **X** represented a set of input parameters for i-th model in the case of both buildings. Additionally, deterministic models with mean material characteristics were used for comparison with stochastic models.

Name of the variable	Mean	COV	Distribution	Ref
Elastic modulus E [MPa]	1620	0.08	Normal	[5]
Shear modulus G [kN/m^2]	625	0.10	Normal	[5]
Compressive strength f_m [MPa]	1.95	0.19	Normal	[5]
Initial shear strength f_{v0} [MPa]	0.153	0.16	Normal	[5]
Friction coefficient μ [-]	0.065	0.12	Normal	[5]
Deformability parameter G_c [-]	7	0.21	Normal	[5]
Softening parameter β [-]	0.3	0.17	Normal	[5]
Shear drift ratio δ_s [%]	0.4	0.10	Normal	Assumed
Flexural drift ratio δ_f [%]	0.8	0.10	Normal	Assumed

Table 2: The statistical characteristics of the input random variables.

3.3 Definiton of near collapse limit-state

The seismic risk was estimated for the near collapse (NC) limit-state, which was at the top displacement that corresponds to the 80% of the building's shear resistance, which is measured in the range beyond the post-capping point of the pushover curve. Definition of more severe limit-state, i.e. the complete collapse of building, was omitted in this study, since numerical model does not consider all phenomena, which occur in extremely nonlinear behaviour of structure.

Note that the NC limit state depends on the ultimate drift ratio, which differs for shear and flexural collapse mechanism and consequently from model to model.

3.4 Acceleration spectrum and seismic hazard

The seismic action is defined with the elastic acceleration spectrum according to the Eurocode 8 - soil type A, which is shown in Figure 4 (left).

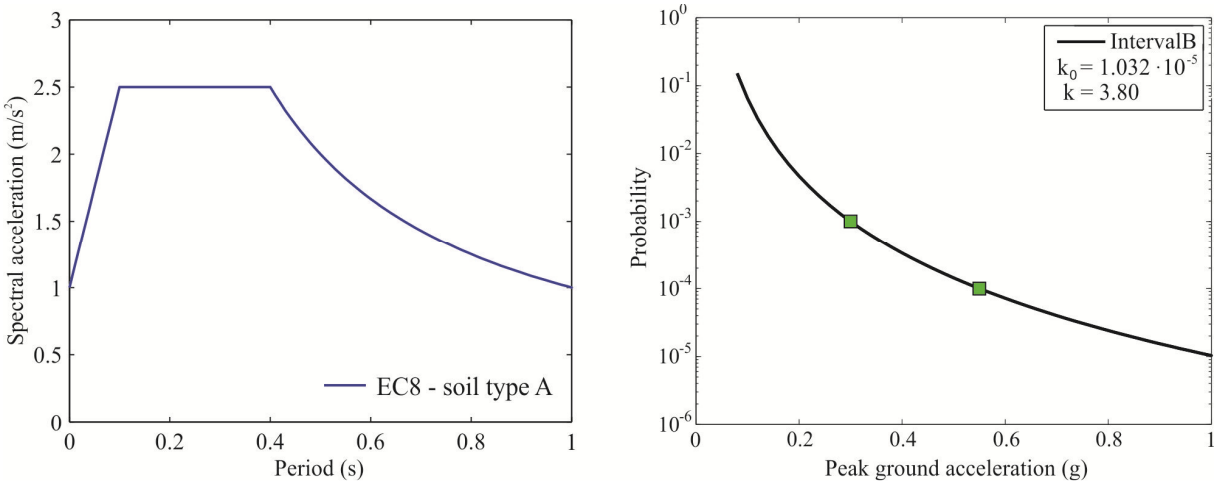

Figure 4: The Eurocode-based acceleration spectrum for soil type A (left) and the hazard curve defined based on the hazard map for return periods of 1000 and 2475 years (right).

The parameters of seismic hazard curve were computed from data, available on the website of the Environment Agency of the Republic of Slovenia [16]. The peak ground accelerations for Ljubljana, soil type A, and return periods of 475 years (10%/50), 1000 years (5%/50) and 2475 years (2%/50), amount to: 0.25 g, 0.30 g and 0.55 g, respectively. Since only two points on the hazard curve are needed in order to calculate parameters k_0 and k (Eq.(2)), it was decided to use the peak ground accelerations corresponding to the return periods of 1000 and 2475 years in order to interpolate the hazard curve in the vicinity of the limit-state intensity $\tilde{a}_{g,LS}$. The resulting curve, which is defined with parameters $k_0 = 1.03 \cdot 10^{-5}$ and $k = 3.8$, is presented in Figure 4 (right).

3.5 Pushover analysis

Pushover analyses for deterministic (mean-valued) model and 30 structural models resulting from LHS technique were performed in Y direction for a building A, and in X direction for a building B, by using the Tremuri [7]. The resulting pushover curves are shown in Figure 5. The force pattern for all pushover analyses was proportional to the product of masses and displacements at first mode shape in the Y direction.

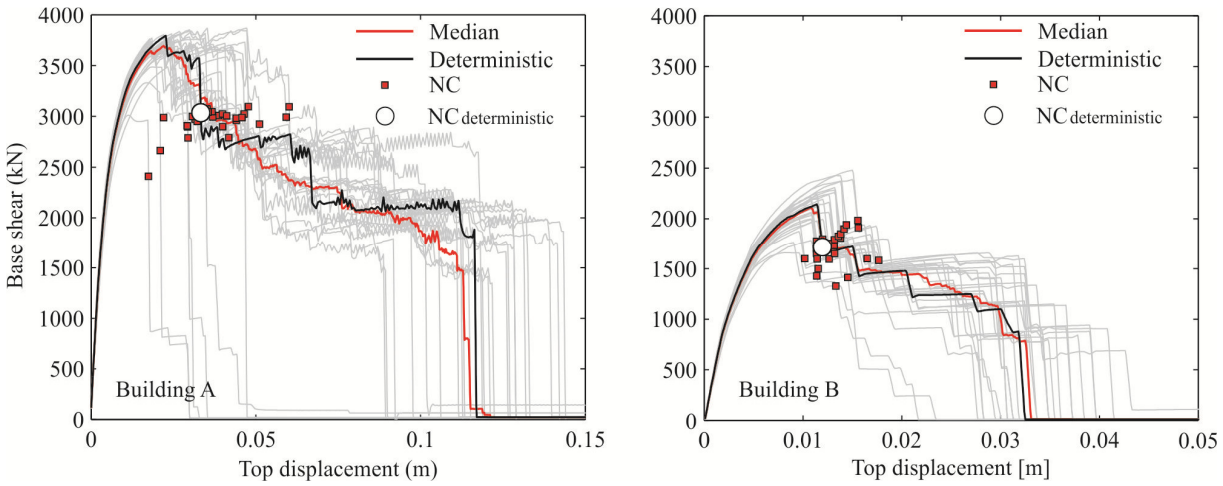

Figure 5: Pushover curves and points indicating the NC limit state for building A (left) and building B (right).

Shear resistance coefficient, which is defined as the ratio between resistance of the building and its weight, has a large value of 0.4 for a building A, and very large value of 0.6 for a building B, due to high percentage of walls in the case of both buildings. In both cases, quite small difference is observed between the median pushover curve, which represents median values of base shear at a given top displacement and the pushover curve of deterministic model.

Red points represent top displacements and corresponding base shears for the NC limit state, which is defined at 80 % of base shear resistance. Similarly, the white circle represents NC limit state of deterministic model. The coefficient of variation of the top displacement at NC limit state for building A is 0.27 and exceeds the coefficient of variation of the corresponding base shear (0.05) for more than five times. The reason for high coefficient of variation of top displacement is not only the high dispersion of the ultimate drift ratios, but also the fact, that uncertainty has the effect on the formation of different plastic mechanisms, which were in this study observed only for building A and are presented in Figures 6, 7 and 8. Different colours in piers represent different failures: red - flexural collapse, yellow - shear collapse and blue - undamaged.

In Figure 6, collapse mechanism of model A8, which occurred at the minimum top displacement ($d_{NC,SDOFA8} = 0.018$ m), is shown. Sudden large drop of base shear observed in the pushover curve is the consequence of simultaneous shear-collapse of several walls in the ground floor (for definition of walls see Figure 2 - left). Such collapse mechanism was expected since the initial shear strength of walls in model A8 is the lowest among these of 30 models and, in addition, the compressive strength and ultimate drift ratios δ_s and δ_f are also low. On the other hand (Figure 7), plastic mechanism of model A27 corresponds to the maximum top displacement ($d_{NC,SDOFA27} = 0.045$ m). At $d_{NC,SDOFA27}$ only a few elements in walls W6 and W13 fail, but at larger displacement, flexural-collapse of all piers in the second storey is observed. In this case, the initial shear strength and ultimate shear-drift ratio are very large, which governs flexural collapse and consequently NC limit-state is attained at larger top displacement. For comparison reasons, plastic mechanism of deterministic model (model A31) is also presented (Figure 8). In this case, structural elements gradually collapse in shear or in flexure at different storeys.

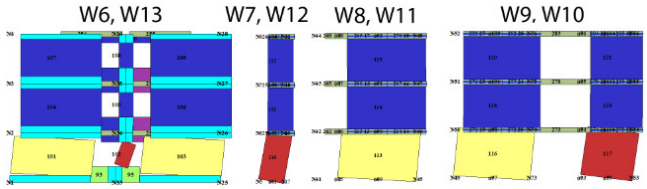

Figure 6: Plastic mechanism corresponding to the NC limit state for Model A8 - minimum top displacement.

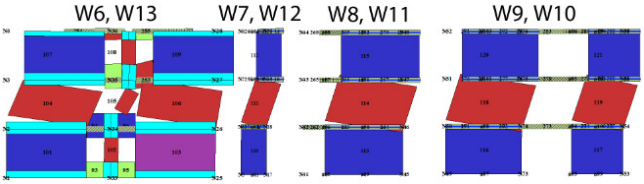

Figure 7: Plastic mechanism corresponding to the NC limit state for Model A27 – maximum top displacement.

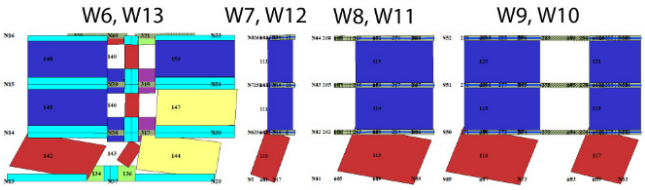

Figure 8: Plastic mechanism corresponding to the NC limit state for deterministic model A31.

In building B, the coefficient of variation in the maximum force at NC limit state is 0.09 and the coefficient of variation of the top displacement is only 0.13, which is much smaller than that obtained for building A. Namely, only one plastic mechanism forms in the case of building B - the soft storey effect in the ground floor. Firstly, element 46 (Figure 9) fails in shear and later other walls in the ground floor collapse in shear or bending. The strength of the element 46 is approximately 20 % of the strength of first storey, therefore it controls the attainment of NC limit state. In some cases the NC limit state is controlled by more than one wall, since the strength of element 46 is less than 20 % of the strength of the first storey. However, variability in NC displacements is relatively small, from 1 cm to 1.77 cm, where the smallest top displacement corresponds to the smallest δ_s.

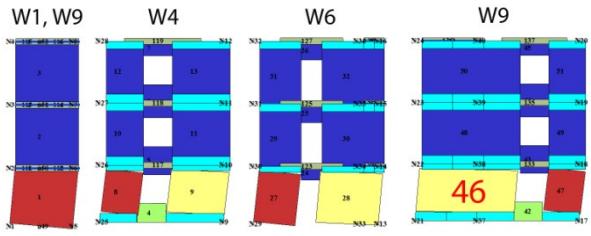

Figure 9: Plastic mechanism corresponding to the NC limit state for model B24.

In order to compute peak ground acceleration that causes the structure to violate the defined NC limit state, pushover curves were idealized using bi-linear force-displacement relationship (Figure 10). It was assumed, that initial stiffness of the equivalent SDOF model is defined based on the pushover curve at 70 % of the base shear resistance. Maximum base shear F_y of the idealized force-displacement relationship is calculated by assuming equal area under the pushover curve and idealized force-displacement relationship, if measured in the interval of displacements from 0 to the displacement d_{NC}, when maximum base shear decreases by 20 % (NC limit state (d_{NC}, F_{NC})). The described idealized force-displacement relationship of pushover curves represents input data for definition of equivalent SDOF model and is shown in Figure 10 for building A.

The force-displacement relationship of equivalent SDOF models were determined by dividing forces and displacements with the transformation factor Γ, having a mean value $\Gamma_{mean,A} = 1.33$ and $\Gamma_{mean,B} = 1.37$ for the building A and B, respectively. The masses of the equivalent SDOF models m^* of building A and B amounted to, respectively, 532 t and 230 t.

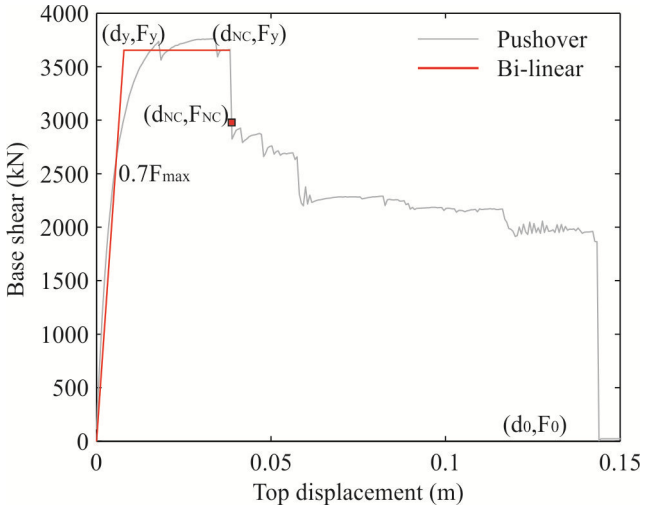

Figure 10: Idealized bi-linear force-displacement relationship of pushover curve.

3.6 Fragility parameters and seismic risk estimation

The fragility parameters were determined by utilizing the N2 method with consideration of epistemic uncertainty. The IN2 curve, as presented in Figure 11, and peak ground acceleration $a_{g,NC}^{IN2}(l)$ were determined for each model of both buildings.

In Table 3 the fragility parameters, estimated based on the procedure described in Section 2, are presented. Median peak ground acceleration and its dispersion were determined with consideration of epistemic uncertainty (U) according to Eqs. (4) and (5).

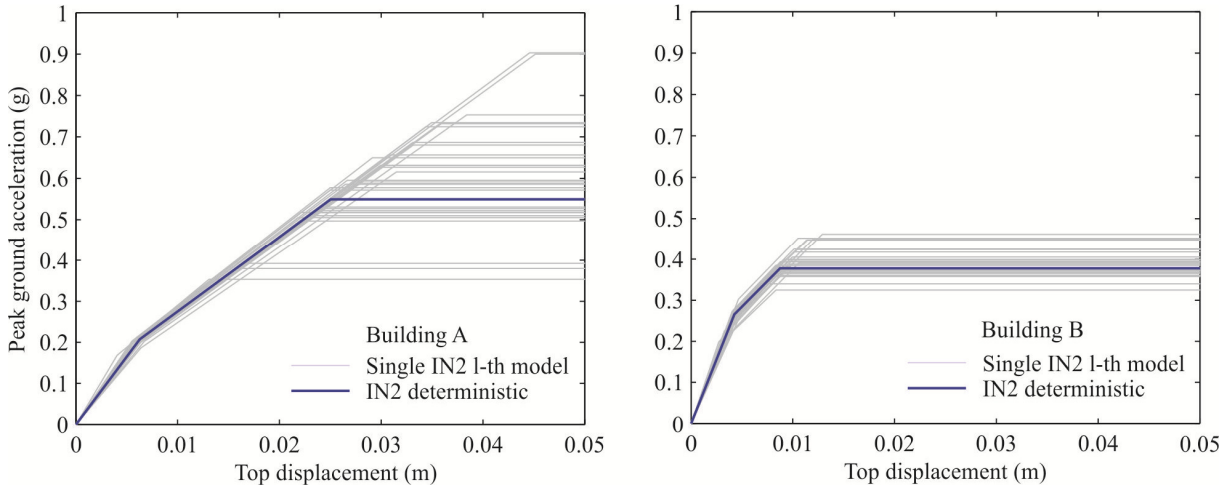

Figure 11: IN2 curves, based on 30 structural models and deterministic model for building A (left) and building B (right).

	Building A				Building B			
Method	$\tilde{a}_g(g)$		β		$\tilde{a}_g(g)$		β	
$IN2_{30}$	$\tilde{a}_{gU,A}^{IN2}$	0.59	$\beta_{U,A}^{IN2}$	0.21	$\tilde{a}_{gU,B}^{IN2}$	0.39	$\beta_{U,B}^{IN2}$	0.08
$IN2_{det}$	$a_{g,\mathrm{det},A}^{IN2}$	0.55	-	-	$a_{g,\mathrm{det},B}^{IN2}$	0.38	-	-

Table 3: The fragility parameters for building A and B.

High estimated median peak ground accelerations, at which the NC limit state is attained, are observed in Table 3, mainly due to the high percentage of walls in both buildings. Further, the peak ground acceleration $\tilde{a}_{g,\mathrm{det},A}^{IN2}$, that corresponds to deterministic model, is slightly smaller than the median peak ground acceleration $\tilde{a}_{gU,A}^{IN2}$, which corresponds to stochastic model. An opposite was observed for building A, if fragility parameters were assessed by conducting nonlinear dynamic analysis for the equivalent SDOF model. However, the difference between $\tilde{a}_{g,\mathrm{det},A}^{IN2}$ and $\tilde{a}_{gU,A}^{IN2}$ is very small.

The dispersions for $\tilde{a}_{gU}^{IN2}$ are 0.21 and 0.08, respectively, for building A and B. Quite small dispersion in the case of building B is the consequence of a small number of different plastic mechanisms that formed in this case. Namely, plastic mechanism affects displacement capacity and consequently the peak ground acceleration that causes the NC limit state.

In the Table 3, only epistemic uncertainties are considered, therefore dispersion due to aleatoric uncertainties β_R has to be assumed and in the case of presented examples equals 0.16. This value was adopted from a previous study, where approximate IDA for a single-degree-of-freedom model of the building A was performed for the 30 ground motion records. The total dispersion β_{RU}^{IN2}, which was used for calculation of seismic risk, was obtained by using SRSS rule as follows:

$$\beta_{RU,A}^{IN2} = \sqrt{\left(\beta_R\right)^2 + \left(\beta_{U,A}^{IN2}\right)^2} = \sqrt{0.16^2 + 0.21^2} = 0.26 \tag{12}$$

$$\beta_{RU,B}^{IN2} = \sqrt{\left(\beta_R\right)^2 + \left(\beta_{U,B}^{IN2}\right)^2} = \sqrt{0.16^2 + 0.08^2} = 0.18 \tag{13}$$

Mean annual frequency of exceeding the NC limit state λ_{NC} ($\mathrm{MAF_{NC}}$), the corresponding return period T_{NC} and the frequency of exceeding NC limit state in 50 years λ_{NC}^{50} are presented in Table 4. $\mathrm{MAF_{NC}}$ for a building B is four times higher than for building A. This is due to

lower capacity of building B in terms of PGA, which has a much higher influence on result (Eq. 3) than dispersion, which is for building B smaller than that of building A.

Building	λ_{NC}	T_{NC}(years)	λ_{NC}^{50} (%)
A	$1.28 \cdot 10^{-4}$	7800	0.64
B	$4.67 \cdot 10^{-4}$	2150	2.31

Table 4: Seismic risk in terms of mean annual frequency of exceeding NC limit state λ_{NC}, corresponding return period T_{NC} and frequency of exceeding NC limit state in 50 years λ_{NC}^{50}.

4 CONCLUSIONS

A simplified method for estimating seismic risk in combination with N2 method was used for determination of fragility parameters in the case of two three-storey masonry buildings. It was shown that the formation of plastic mechanisms has a significant effect on the estimation of fragility parameters. If only one plastic mechanism controls the seismic response of the building, the dispersion for $\tilde{a}_{gU}^{IN2}$ and the dispersion in drift capacity of the wall, which is an input parameter, are almost the same. This is not true for building A, where several plastic mechanisms were observed from pushover analyses. Since it is difficult to judge in advance, whether the modeling uncertainties affect plastic mechanism or not, it is also difficult to prescribe the dispersion measures. Therefore the use of simplified methods, which enable fast estimation of effects of epistemic uncertainties on seismic response parameters, may become more often used for risk assessment of masonry buildings.

ACKNOWLEDGEMENTS

The results presented in this paper are based on the work partially supported by the Slovenian Research Agency. The work of the first author, young researcher at ELEA iC d.o.o., was partially supported by the European Union, from the European Social Fund. This support is gratefully acknowledged.

REFERENCES

[1] C.A. Cornell, F. Jalayar, R.O. Hamburger, D.A. Foutch. Probabilistic basis for 2000 SAC Federal Emergency Management Agency Steel Moment Frame Guidelines. *Journal of Structural Engineering ASCE*, 128, 526-533, 2000.

[2] D. Vamvatsikos, C.A. Cornell. Incremental Dynamic Analysis. *Earthquake Engineering and Structural Dynamics*, 31, 491-514, 2002.

[3] M. Dolsek and P. Fajfar. Simplified probabilistic seismic performance assessment of plan-asymmetric buildings. *Earthquake Engineering and Structural Dynamics*, 36, 2021-2041, 2007.

[4] P. Fajfar. A nonlinear analysis method for performance-based seismic design. *Earthquake Spectra*, 16, 573-592, 2000.

[5] M. Rota, A. Penna, G. Magenes. A methodology for deriving analytical fragility curves for masonry buildings based on stochastic nonlinear analyses. *Engineering Structures, Early View, doi:10.1016/j.engstruct. 2010.01.009,* 2010.

[6] M. Vořechovský, D. Novák. Statistical correlation in stratified sampling. *Proc. Of 9th Int. Conf. On Applications of Statistics and Probability in Civil Engineering – ICASP 9, San Francisco, USA, Rotterdam Millpress*: 119-124, 2003.

[7] A. Galasco, S. Lagomarsino, A. Penna. Tremuri program: Seismic analyses of 3d masonry buildings. *Italy - University of Genoa,* 2009.

[8] M. Dolsek. Incremental dynamic analysis with consideration of modeling uncertainties. Earthquake Engineering and Structural Dynamics, 38, 805-825, 2009.

[9] M. Dolsek. Simplifed method for seismic risk assessment of buildings with consideration of aleatoric and epistemic uncertainty. *Submitted in Structure and Infrastructure Engineering*, 2010.

[10] M.D. McKay, W.J. Conover, R.J. Beckman. A Comparison of Three Methods for Selecting Values of Input Variables in the Analysis of Output from a Computer Code. *Technometrics*, 21: 239–245, 1979.

[11] S. Frumento, G. Magenes, P. Morandi, G.M. Calvi. Interpretation of experimental shear tests on clay brick masonry walls and evaluation of q-factors for seismic design. *EUCENTRE and University of Pavia,* 2009.

[12] ELSA - SPEAR seismic performance assessment and rehabilitation of existing buildings. *European Laboratory for Structural Assessment, Ispra*. http://elsa.jrc.ec.europa.eu/term_activity.php?id=2, 2005.

[13] S.T.A. Data. 3Muri 4.0.0. – User manual. *http://www.3muri.com/3muri/documenti/3Muri4.0_User_Manual.pdf, 2009.*

[14] A. Penna. A macro-element procedure for the non-linear dynamic analysis of masonry buildings. Ph.D. dissertation [*in Italian*]. *Italy - Politecnico di Milano*, 2002.

[15] M. Tomazevic. Potresno odporne zidane stavbe. *Ljubljana, Tehnis*, 2009.

[16] Environment Agency of the Republic of Slovenia, *http://www.arso.gov.si/potresi/potresna%20nevarnost/*, dec 2010.